MCM4 mutation causes adrenal failure, short stature, and natural killer cell deficiency in humans

Claire R. Hughes,[1] Leonardo Guasti,[1] Eirini Meimaridou,[1] Chen-Hua Chuang,[2] John C. Schimenti,[2] Peter J. King,[1] Colm Costigan,[3] Adrian J.L. Clark,[1] and Louise A. Metherell[1]

[1]Queen Mary University of London, Centre for Endocrinology, William Harvey Research Institute, Barts and the London School of Medicine and Dentistry, London, United Kingdom. [2]College of Veterinary Medicine, Cornell University, Ithaca, New York, USA. [3]Paediatric Endocrinology and Diabetes, Our Lady's Children's Hospital, Dublin, Ireland.

An interesting variant of familial glucocorticoid deficiency (FGD), an autosomal recessive form of adrenal failure, exists in a genetically isolated Irish population. In addition to hypocortisolemia, affected children show signs of growth failure, increased chromosomal breakage, and NK cell deficiency. Targeted exome sequencing in 8 patients identified a variant (c.71-1insG) in minichromosome maintenance–deficient 4 (*MCM4*) that was predicted to result in a severely truncated protein (p.Pro24ArgfsX4). Western blotting of patient samples revealed that the major 96-kDa isoform present in unaffected human controls was absent, while the presence of the minor 85-kDa isoform was preserved. Interestingly, histological studies with *Mcm4*-depleted mice showed grossly abnormal adrenal morphology that was characterized by non-steroidogenic GATA4- and Gli1-positive cells within the steroidogenic cortex, which reduced the number of steroidogenic cells in the zona fasciculata of the adrenal cortex. Since MCM4 is one part of a MCM2-7 complex recently confirmed as the replicative helicase essential for normal DNA replication and genome stability in all eukaryotes, it is possible that our patients may have an increased risk of neoplastic change. In summary, we have identified what we believe to be the first human mutation in *MCM4* and have shown that it is associated with adrenal insufficiency, short stature, and NK cell deficiency.

Introduction

Familial glucocorticoid deficiency (FGD) is an autosomal recessive form of adrenal failure characterized by adrenocorticotropic hormone–resistant (ACTH-resistant) isolated glucocorticoid deficiency (1, 2). This disease is relatively common in the Irish Traveler community, a genetically isolated population with high levels of consanguinity (3). In addition to adrenal insufficiency, patients also have evidence of increased chromosomal breakage, NK cell deficiency, and growth failure. Seven children with adrenal failure from 3 kindreds within the Irish Traveler community were studied (Figure 1A), with clinical features summarized in Table 1. Patients have typical biochemical features of FGD, with isolated glucocorticoid deficiency, raised ACTH, and normal renin and aldosterone. All children are maintained on replacement hydrocortisone, 10–14 mg/m²/d. Unlike other forms of FGD, cortisol deficiency is often not as severe and onset is usually in childhood following a period of normal adrenal function. Patient 8 (Table 1) has not at the time the present study was concluded developed adrenal failure but has evidence of short stature, increased chromosomal fragility, and NK cell deficiency. Four children have evidence of increased chromosomal breakage on screening with diepoxybutane. Three children have levels of breakage consistent with Fanconi anemia but no other dysmorphic features characteristic of this or any other DNA repair disorder. All continue to have a normal full blood count, with no evidence of abnormality apart from the specific NK deficiency. Children had a low birth weight and are currently notably short compared with their mid-parental height standard

deviation score (SDS), despite a normal growth hormone/IGF-1 axis. Seven children have low levels of NK cells, although only one patient demonstrates increased susceptibility to infection; patient 6 has had recurrent pneumonitis and has evidence of bronchiectasis on CT of the chest. Known causes of adrenal insufficiency were excluded clinically and biochemically, and mutations in *MC2R*, *MRAP*, and *STAR*, all associated with FGD, were not detected. Since the clinical features cosegregated and inheritance patterns were suggestive of autosomal recessive mechanisms, we sought common areas of homozygosity and subsequently interrogated these areas using exon capture and high-throughput sequencing.

Results

SNP array genotyping with the GeneChip Mapping 10K array and analysis with IBDfinder identified three areas of homozygosity common to 5 affected patients, two on chromosome 8 totaling 17.5 Mb (8p12–8q11.22 and 8q12.2–q12.3) and one of 4 Mb on chromosome 4q22.3–23 (Figure 1B). Genotyping of microsatellite markers confirmed homozygosity in the pericentric region on chromosome 8 in affected family members (Figure 1B). Exon capture and high-throughput sequencing of all three regions was carried out in one patient, identifying 680 variants from the 2009 human reference sequence (GRCh37/hg19). We reduced the number of variants to 3 by evaluating non-synonymous coding variants, splice variants, and indels and by excluding variants that were heterozygous or annotated in SNP databases (Ensembl SNP database, release 54). These three variants were then sequenced in other affected patients from the Irish Traveler community, their parents, and unaffected controls. Only one variant, c.71-1insG in minichromosome maintenance–deficient 4 (*MCM4*), was homo-
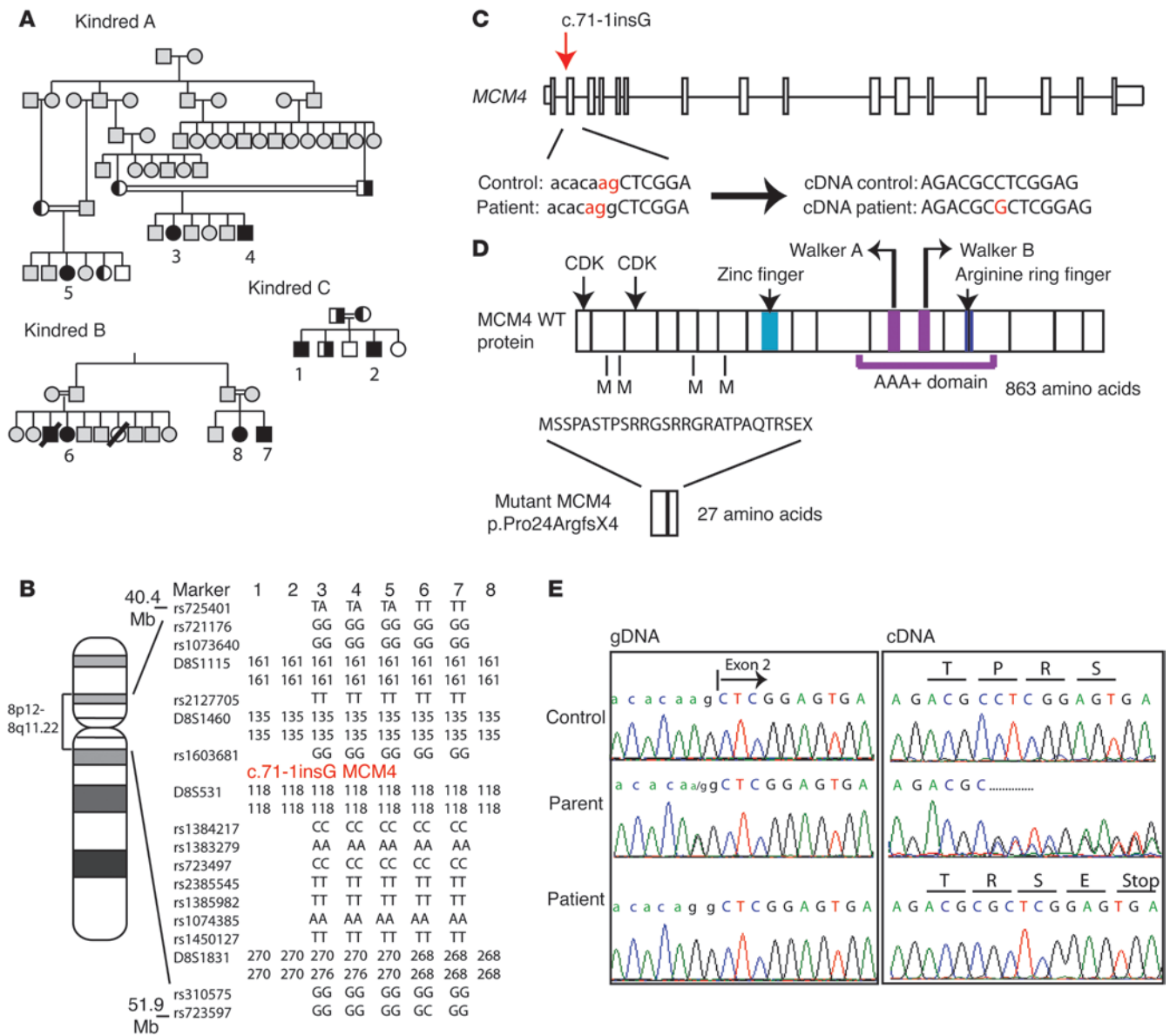
Figure 1
Pedigree and linkage analysis of 3 affected kindreds and identification of a mutation in *MCM4* leading to a truncated protein p.Pro24ArgfsX4. (**A**) Pedigree of affected patients. (**B**) SNP and microsatellite genotyping of chromosome 8p12.2–q12.3 locus surrounding *MCM4*. Genotyping was not carried out on patients 1, 2, and 8. (**C**) Gene structure of *MCM4* (top). The location of the mutation, c.71-1insG, prior to exon 2 (red arrow), which leads to a shift in the consensus splice site (nucleotides ag in red) and the introduction of an extra G into patient mRNA/cDNA (shown below), is indicated. (**D**) Protein structure of MCM4 indicating (top) the positions of the two cyclin-dependent kinase (CDK) binding domains, zinc finger, Walker A and B motifs, and an arginine ring finger; these motifs are conserved across all MCMs and are essential for MCM4 functionality. Also indicated are 4 in-frame methionines (M). The predicted consequence of the c.71-1insG mutation leading to premature truncation of the protein at amino acid 27 (p.Pro24ArgfsX4) is shown (bottom). (**E**) Partial sequence chromatograms showing (left) the intron 2–exon 2 junction in genomic DNA from control, parent, and patient (intronic bases in lowercase, exonic in uppercase). Arrows indicate the base change from A to G and (right) cDNA from control, parent, and patient indicating wild-type, mixed, and mutant cDNA sequences, respectively, the latter resulting in a premature stop codon.

zygous in all 8 affected patients and segregated with the disease. (Figure 1, A and E). The two other variants in ankyrin 1 (*ANK1*) and ADAM metallopeptidase domain 5, pseudogene (*ADAM5P*) were subsequently recognized as SNPs (rs117614251 and rs73612404, respectively). In kindreds A and C, parents were heterozygous for the *MCM4* variant, and all siblings tested had either heterozygous

or homozygous wild-type sequences (parental and sibling samples were not available for kindred B). This variant (maximum lod score of 8.4) was not present in SNP databases and was not seen in 1000 Genomes (4), the NHLBI Exome Sequencing Project (>10,700 alleles sequenced), or on screening of 300 control chromosomes of individuals of European descent.

Table 1
Clinical phenotype of patients included in study

Patient	Age at diagnosis of adrenal insufficiency (yr)	Presenting complaint	9 a.m. cortisol (nmol/l) NR >200	ACTH at diagnosis (ng/l) NR 9–52	Maximum cortisol with ACTH stimulation NR >550	Birth weight SDS	Current height SDS	MPH SDS	Chromosomal breakage[A]	NK cell levels NR 200–300 (9%–16%)[B]
1	2.5	FTT/pigmented	112	265	314	−3.0	−3.3	0.2	7 breaks, 1 exchange	210 (5%)
2	12	Short stature/screened	167	50	356	−1.8	−2.1	0.2	3 breaks, 2 exchanges	–
3	7.9	FTT/pigmented	114	259	–	−2.1	−1.4	0.1	8 breaks	60 (2%)
4	0.5[C]	FTT/pigmented	244	156	325	−2.3	−2.3	0.1	13 breaks, 4 exchanges	78 (3%)
5	5	Hypoglycemia/pigmented	<20	439	–	–	−1.1	0.8	22 breaks, 8 exchanges	29 (1.4%)
6	4.5	Hypoglycemia/pigmented	308	195	308	−2.2	−1.3	1.1	–	27 (2%)
7	0.5[C]	FTT	229	126	364	−2.0	−3.4	−0.4	21 breaks, 5 exchanges	18 (1.1%)
8	–	FTT	210	27	577	−1.9	−2.6	−0.4	152 breaks, 54 exchanges	141 (3%)

[A]Lymphocytes treated with 0.1 mcg per ml diepoxybutane for duration of culture, normal background up to 8 breaks/2 exchanges per test (80 cells quantified). [B]The absolute NK cell count (measured in cells/mm³ of whole blood) and the percentage of lymphocytes that were NK cells in the first whole-blood sample analyzed are indicated for each individual tested. [C]Screened due to positive family history. Patient 8 (aged 4 years) was included because she has short stature, increased chromosomal fragility, and NK cell deficiency; however, she has not at the time of the present study was concluded developed adrenal insufficiency. NR, normal range; MPH, mid-parental height; FTT, failure to thrive.

This variant, a splice site mutation, altered the consensus sequence and would be predicted to shift the splice acceptor site upstream by one nucleotide and lead to a frameshift and a foreshortened open reading frame encoding a prematurely terminated translation product (p.Pro24ArgfsX4). The splice site shift was confirmed by performing RT-PCR on total RNA from whole blood isolated from two patients, a heterozygous relative, and an unaffected control (Figure 1, D and E).

Cell lysates from peripheral blood lymphocytes from unaffected human controls were immunoblotted for MCM4. This identified two major proteins migrating at approximately 96 kDa and 85 kDa. Patient samples showed only one major MCM4 species at 85 kDa (Figure 2A), suggesting an alternative transcription or translation start site may be present to explain the 85-kDa form. To our knowledge, no alternative splice variant has been reported that would explain this smaller MCM4 species.

cDNA encoding full-length MCM4 with a C-terminal HA tag was generated by PCR and cloned into an expression vector, and the initiating methionine was mutated using site-directed mutagenesis (M1X). Wild-type and/or M1X constructs were transiently expressed in HEK293 cells, and cell lysates were immunoblotted with HA and MCM4 antibody. M1X expression resulted in a smaller MCM4 species of approximately 85 kDa that corresponded in size to that seen in patient samples (Figure 2B).

cDNAs encoding proteins beginning at the first, second, and third in-frame ATGs (Figure 2C) were generated by PCR, then cloned, transfected into HEK293 cells, and immunoblotted. The first and third in-frame ATGs produced proteins corresponding in size to those seen in vivo, suggesting that the faster-migrating protein observed in patients may result from internal initiation from the third in-frame ATG (Figure 2C). This protein was also seen in a number of human cell lines (Figure 2D) but was not detected by immunoblotting with an N-terminal antibody for MCM4, suggesting this smaller MCM4 protein lacks the N terminus (Figure 2D). In patient samples and human cell lysates, the smaller band appeared to be a doublet. This may be due to phosphorylation, as there is evidence for multiple phosphorylation sites on MCM4 (4, 5).

Adrenal glands from affected patients were not available for study. In mice, homozygosity for a disrupted *Mcm4* allele (*Mcm4*−/−) caused pre-implantation lethality. A hypomorphic allele of *Mcm4*, chromosome aberrations occurring spontaneously (*Chaos3*), leads to genomic instability and cancer (6), but *Mcm4*Chaos3/− embryos died late in gestation. However, the near 100% lethality of *Mcm4*Chaos3/− is rescued by *Mcm3* heterozygosity (7), and these animals provide the closest viable animal model to our patient cohort, in that MCM4 levels were reduced to the lowest levels compatible with life. Adrenals from 3.5-month-old *Mcm4*Chaos3/−*Mcm3*+/− mice were of normal size, but H&E staining revealed an abnormal morphology characterized by small, tightly packed, intensely stained spindle-shaped cells in the cortex just beneath the capsule that appeared to be migrating into the cortex (Figure 3, E and F). By 12 months of age, these cells were abundant and in some areas spanned the cortex from the capsule to the medulla (Figure 3, G and H). Such changes were not observed in wild-type littermate controls (Figure 3B), in *Mcm4*Chaos3/+*Mcm3*+/− adrenals (Figure 3, C and D), or in other organs of the *Mcm4*Chaos3/−*Mcm3*+/− mice (7). The adrenal capsule adjacent to these abnormal cells appeared to be much thinner, which is particularly obvious in the higher-power images (compare Figure 3, I and J). Analysis of the expression of steroidogenic enzymes indicated many cells in the mutants were negative for CYP11A1 (P450 side chain cleavage [SCC]) (Figure 3L), in contrast to the wild-type (Figure 3K). Co-staining with the zona fasciculata marker CYP11B1 (P450 11β-hydroxylase) showed that these CYP11A1-negative cells were also CYP11B1 negative (Figure 3P), implying they were not capable of producing glucocorticoid. These cells were also GATA-4 positive (Figure 3R); GATA-4 is a transcription factor that is not usually expressed in the adult adrenal (Figure 3Q and ref. 8). The juxtaposition of the thinning capsule and the nonsteroidogenic cells in the mutant adrenals suggested that these cells might be capsular in origin. Expression of the mesenchymal capsule marker Gli1 was analyzed by in situ hybridization, which indicated that the abnormal cells were Gli1 positive (Figure 3U). Taken together, these data indicate that the adrenal morphology in this MCM4 depletion mouse model is grossly abnormal, with steroidogenic cells displaced by non-steroidogenic, GATA-4– and Gli1-positive cells that are likely to compromise steroidogenic output.
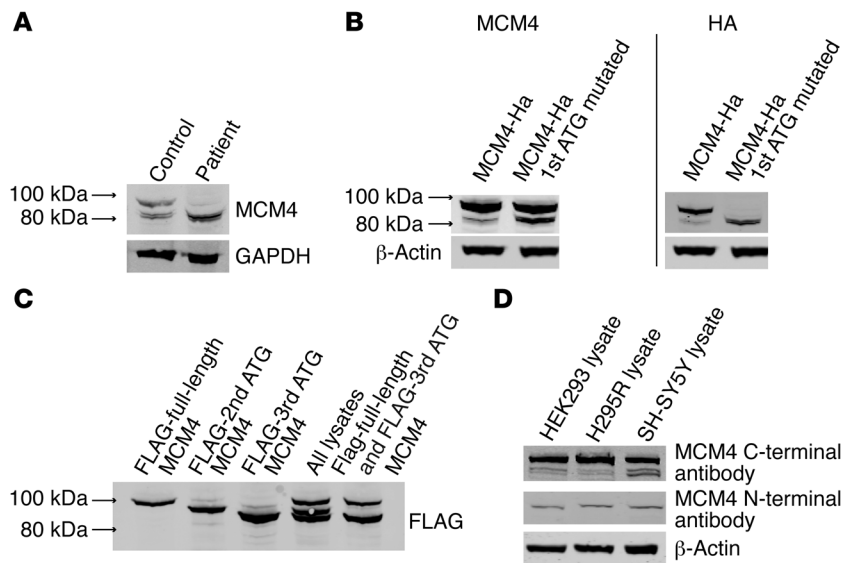
Figure 2
Cell lysates from both control and patient lymphocytes show evidence of MCM4 protein.
(**A**) Lysates from patient and control human lymphocytes were immunoblotted with an anti-MCM4 antibody. While control subjects have two main protein species, of approximately 96 and 85 kDa, the predicted full-length 96-kDa product is missing in the patients. (**B**) HEK293 cells were transfected with full-length MCM4 or MCM4 with the first methionine mutated, both of which were tagged with a C-terminal HA tag. The lysates were then blotted with both MCM4 antibody (left panel) and HA antibody (right panel). Abolition of the initiating methionine of MCM4 leads to expression of a smaller MCM4 species, of approximately 85 kDa. (**C**) FLAG-tagged full-length MCM4 and constructs beginning at the second and third in-frame ATGs were expressed in HEK293 cells. Lysates from each were run individually (lanes 1–3), all together (lane 4), or in combination with the full-length and third ATG (lane 5) and immunoblotted using an anti-FLAG antibody. The relative mobility of the different species indicates that the smaller MCM4 species may be produced by translation from the third in-frame ATG. (**D**) Different cell lysates show evidence of both the major full-length and smaller MCM4 isoforms when immunoblotted with the MCM4 C-terminal antibody. However, when the same lysates are immunoblotted with the N-terminal antibody, the smaller MCM4 isoform is no longer seen, suggesting that the smaller isoform is missing the N terminus of MCM4.

Discussion

We have demonstrated that a mutation in *MCM4* in a cohort of patients from the Irish Traveler community leads to adrenal insufficiency, short stature, and NK cell deficiency. Given the essential role MCM4 plays in cell division, it may be surprising that this mutation, causing early termination of the reading frame, should produce such a mild phenotype when gene knockout in mice is embryonic lethal. Immunoblotting of patient lymphocytes showed loss of the full-length 96-kDa MCM4 protein as predicted from RNA analysis but showed evidence of a smaller, 85-kDa MCM4 isoform. We propose that this smaller isoform rescues the patients from a lethal phenotype. Given the location of the mutation and the fact that the antibody used in this experiment detects the C terminus of MCM4, it is probable that this smaller isoform has a disrupted N-terminal domain in these patients, but the essential conserved C-terminal domains remain intact. The N terminus is not well conserved, and studies have revealed that deletion of the first 130 aa is not deleterious in eukaryotic cells (9). Further work has also suggested that although the eukaryotic N-terminal domain is non-essential, it is involved in protein kinase regulation of cell cycle progression (10). Budding yeast engineered to express

the orthologous *Chaos3* hypomorphic allele showed DNA replication defects and genomic instability (11, 12). In addition to the abnormal adrenal phenotype, $Mcm4^{Chaos3/-}Mcm3^{+/-}$ mice also have high levels of genomic instability, indicated by elevated micronuclei in red blood cells, which correlates with the chromosomal fragility seen in our patients. Furthermore, they exhibit severe growth failure and increased susceptibility to the development of, primarily, mammary tumors, histiocytic sarcomas, and lymphomas, depending on genetic background (7). We have not detected any form of cancer in our patients, but suggest that they may have an increased risk of neoplastic change.

Some features of the mutant adrenal histology have been described in murine adrenal hyperplasia (13–15). The hyperplastic cells in these mouse models are morphologically very similar to those we observe, and are also GATA-4 positive and non-steroidogenic. The presence of these non-steroidogenic cells in the cortex reduces the number of steroidogenic CYP11B1-expressing cells and hence presumably the glucocorticoid output of the zona fasciculata. The adrenal cortex is a dynamic organ that is constantly remodeling to maintain homeostasis. It is proposed that it does this by recruiting differentiated steroidogenic cells into the zona fasciculata or zona glomerulosa from stem/progenitor cell populations (16, 17). One such population has been characterized in the mesenchymal adrenal capsule with, at least during development, Gli1-expressing cells delaminating from the capsule and entering the cortex, concomitantly extinguishing Gli1 expression and activating SF-1 and CYP11A1 expression to become steroidogenic (16). In light of this, it is interesting to note that the GATA-4–positive, non-steroidogenic, cells also express Gli1, suggesting that they may be capsule cells that enter the cortex but fail to differentiate into a steroidogenic identity, instead activating GATA-4 expression. This is supported by the observation that the capsule appears to be thin adjacent to the regions of infiltration, further suggesting that over time the rate of infiltration exceeds the ability of the capsule to self-renew. Depletion of MCMs has been proposed to lead to stem cell defects in mice (7, 18), with lower MCM2 levels associated with reduced numbers of stem cells in the subventricular zone, skeletal muscle, and intestinal crypts in adult mice. Similarly, the relatively specific impingement of the MCM4 defect on adrenal function may be a consequence of its effect on the growth of these mesenchymal stem/progenitor cells and their differentiation into steroidogenic cells. This suggests MCM4 may have additional functionality beyond DNA replication.

Complete NK cell deficiency in humans is rare, with the few cases reported resulting in overwhelming and fatal infection during childhood (19). The children in our cohort clearly have low but not absent NK cell levels, and only one patient demonstrates increased susceptibility to infection. An accompanying article reports the detailed characterization of the NK cell defect resulting from this mutation (20).
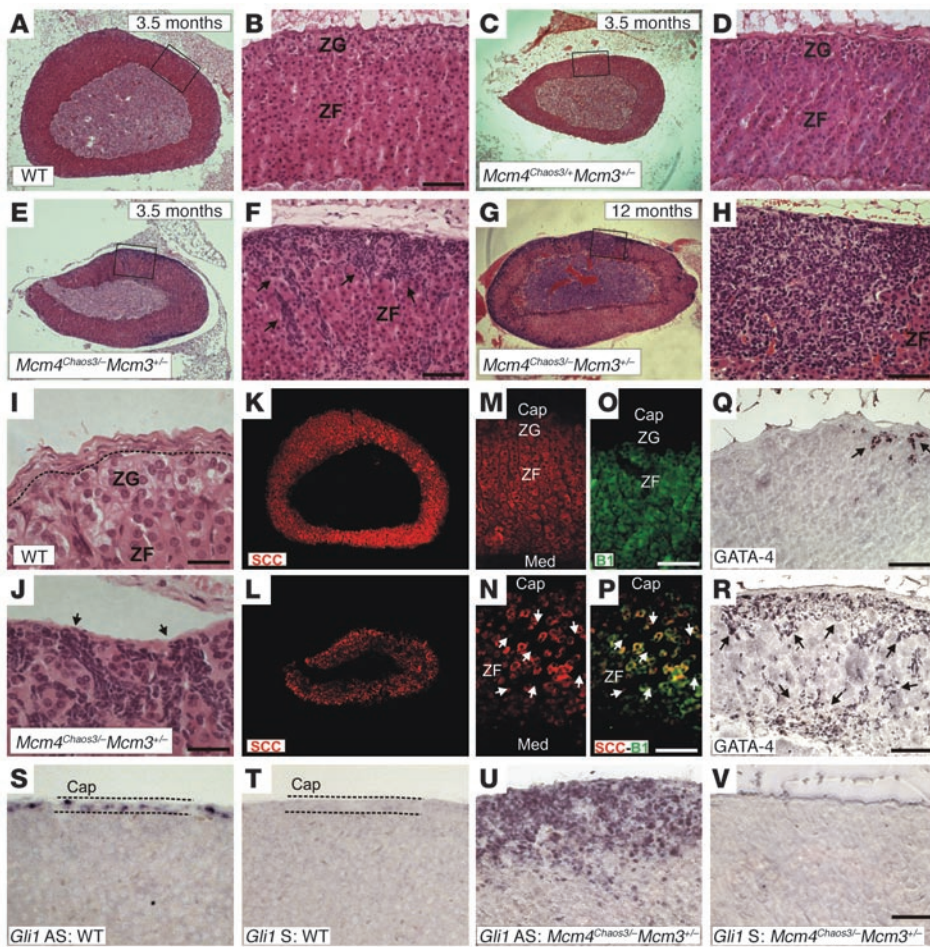
Figure 3
Analysis of adrenals from MCM4 mutant mouse models. (**A–J**) Adrenal cortices of *Mcm4^Chaos3/−^Mcm3^+/−^* mice have an abnormal morphology. H&E staining of wild-type (**A**, **B**, and **I**), *Mcm4^Chaos3/+^Mcm3^+/−^* (**C** and **D**), and *Mcm4^Chaos3/−^Mcm3^+/−^* adrenals at 3.5 months (**E** and **F**) and *Mcm4^Chaos3/−^Mcm3^+/−^* at 12 months (**G**, **H**, and **J**). Atypical spindle-shaped cells are observed within the cortex in the *Mcm4^Chaos3/−^Mcm3^+/−^* adrenals 3.5 months (arrows in **F**), with a more severe phenotype at 12 months (**H**). The normal capsule architecture in the wild-type (**I**) is lost adjacent to the abnormal cells (**J**). (**K–V**) Atypical cells in the cortex are not steroidogenic. 3.5-month-old wild-type (**K**, **Q**, and **S**) and *Mcm4^Chaos3/−^Mcm3^+/−^* (**L**, **R**, and **U**) adrenals were stained for P450 SCC (**K**, **L**, **M**, and **N**), CYP11B1 (B1) (**O**), double SCC-B1 (**P**), and GATA-4 (**Q** and **R**). The atypical cells populating the zona fasciculata in *Mcm4^Chaos3/−^Mcm3^+/−^* adrenals are negative for both SCC and CYP11B1 (arrows in **N** and **P**). GATA-4 immunoreactivity was rarely observed in the wild-type adrenals and always in cells close to the capsule (arrows in **Q**). In *Mcm4^Chaos3/−^Mcm3^+/−^* samples, the atypical cells are GATA-4 positive (arrows in **R**). In situ hybridization on 12-month-old adrenals showed that Gli1 expression is restricted to the capsule in the wild-type (**S**) but detected in the cortex in the atypical cells in *Mcm4^Chaos3/−^Mcm3^+/−^* mice (**U**). T and V are sense probe controls. Cap, capsule; Med, medulla; ZF, zona fasciculata; ZG, zona glomerulosa. Scale bars: 100 μm (**A–H**, **K–V**), 40 μm (**I** and **J**).

of the pre-replicative complex, which licenses origins for DNA synthesis in the S phase (4, 21). Recently, 5 genes that encode different components of the pre-replicative complex have been implicated in Meier-Gorlin syndrome (22), which includes pre- and postnatal growth failure. Taken together, the findings indicate that defects in replication licensing might lead to disorders with similar growth retardation phenotypes but distinct developmental abnormalities. The other components of the MCM complex therefore represent prime potential candidates for other undiagnosed cases of chromosomal instability or adrenal failure.

Methods

Mutation discovery

PCR and sequencing. Genomic DNA was extracted from peripheral blood leukocytes, and each exon of genes of interest including intronic boundaries was amplified by PCR using specific primers (for these and all subsequent primer sequences, see Supplemental Table 1; supplemental material available online with this article; doi:10.1172/JCI60224DS1). The reaction mixture contained 100 ng of DNA template, 1× PCR buffer, 200 μM each dNTP, 200 nM each primer, and 1 U *Taq* DNA polymerase (Sigma-Aldrich). Cycling conditions were 95°C for 5 minutes (1 cycle); 95°C for 30 seconds, 55°C for 30 seconds, and 72°C for 30 seconds (30 cycles); and 72°C for 5 minutes. PCR products were visualized on 1% agarose gel and sequenced using the ABI Prism BigDye sequencing kit and an ABI 3700 automated DNA sequencer (Applied Biosystems), in accordance with the manufacturer's instructions.

Genome-wide SNP array. For the whole-genome scan, the GeneChip Mapping 10K array *Xba131* (Affymetrix) was used in accordance with the manufacturer's guidelines as previously described (23). This version of the Mapping 10K array comprises a total of 11,555 SNPs, with a mean inter-marker distance of 210 kb, equivalent to 0.32 cM. SNP genotypes were scanned for regions of homozygosity using IBDfinder from the Centre for Autozygosity Mapping (http://autozygosity.org and ref. 24).

Sequence capture array and sequencing. A custom sequence capture array targeting the exons 50 bp up- and downstream plus 1 kb upstream of the transcription start site for each RefSeq gene within the areas of homozygosity (coordinates 4:96.3–100.3, 8:36.8–51.9, and 8:62.1–64.5) was designed and manufactured by Roche NimbleGen. A 472-fold enrichment of the targeted regions was achieved, and sequencing was performed on a single

In conclusion we have identified a mutation in *MCM4* characterizing a what we believe to be a new DNA replication disorder. Patients demonstrate a phenotype similar to other DNA repair and replication disorders, including increased chromosomal fragility, pre- and postnatal growth retardation, and variable immune deficiency; in addition, this disorder includes adrenal insufficiency. Patients exhibit variability not only in disease susceptibility but also in the other features of the syndrome, including age of onset of adrenal insufficiency, NK deficiency, and levels of chromosome breakage. MCM4, as a component of the MCM2-7 complex, is part

lane of the Illumina Genome Analyzer II. SNPs, with a threshold coverage of at least 10 reads on the respective nucleotide, were called with the MAQ alignment and downstream analysis tools. The results were checked against the Ensembl SNP database, release 54.

Validation. We reduced the number of variants for validation by the following strategy: (a) considering candidate exons within the disease-linked loci only; (b) excluding variants that were heterozygous; (c) removing variants annotated in SNP databases (Ensembl SNP database, release 54); and (d) evaluating non-synonymous coding SNPs, splice variants, and indels only. The validity of all putative variants in the targeted regions was tested by PCR amplification and sequencing (as above) of the variant position in all 8 patient samples, their parents, and controls.

Genotyping
PCR products (PCR method as above) for *MCM4* exon 2 were digested by AluI restriction digest. AluI cleaves the PCR product from a wild-type sequence once but does not cut the mutant sequence. PCR product (10 μl) was incubated with 10 U AluI (New England BioLabs) in a 30-μl reaction at 37°C for 2 hours. Digestion products were resolved on a 2% agarose gel. Control samples gave rise to 2 bands following digestion; PCR products from DNA with c.71-1insG were not digested and remained as 1 band; heterozygotes resulted in 3 bands.

RNA extraction and cDNA sequencing
Total RNA was isolated and purified from patient and control leukocytes using the PAXgene Blood RNA (QIAGEN) system. The RNA was reverse transcribed and the resulting cDNA used as a template for PCR amplification and sequencing of *MCM4* exons 2–4.

Leukocyte separation, vector construction, and immunoblotting
Fresh whole blood was collected into sample tubes containing EDTA. Mononuclear cells were extracted using a gradient density centrifugation method with Histopaque-1077 as per the manufacturer's protocol (Sigma-Aldrich). Cells were lysed by addition of RIPA buffer (50 mM Tris-HCl, pH 8.0, with 150 mM sodium chloride, 1% IGEPAL CA-630 [NP-40], 0.5% sodium deoxycholate, and 0.1% sodium dodecyl sulfate), supplemented with complete, Mini, EDTA-free Protease Inhibitor Cocktail Tablets (Roche) on ice for 30 minutes. Samples were then centrifuged at 15,000 *g* for 12 minutes at 4°C, and the supernatant was added to Laemmli loading buffer.

Expression constructs
FLAG-MCM4 constructs were prepared using human *MCM4* cDNA (Source Bioscience), which was cloned into a p3xFLAG-CMV10 expression vector (Sigma-Aldrich) after PCR amplification. *MCM4* cDNAs from the second and third in-frame ATGs were amplified using specific primers and cloned into the same p3xFLAG-CMV10 expression vector (Sigma-Aldrich). Alternatively, PCR amplification generated MCM4 with a C-terminal HA tag, which was then cloned into an expression vector. The initiating methionine was mutated using site-directed mutagenesis. The sequence of all constructs was verified by DNA sequencing.

Cell culture and transfections
HEK293T cells were maintained in DMEM with 10% FCS and 1% penicillin/streptomycin. H295R cells were maintained in DMEM/F12 (1:1) supplemented with F12, 2% NuSerum (BD), insulin-transferrin-selenium (ITS), and penicillin/streptomycin. Transient transfections were carried out using Lipofectamine 2000 (Invitrogen) according to the manufacturer's instructions. Total plasmid DNA amounts were kept constant. Whole-cell lysates were prepared 24 hours after transfection. Cells were washed 3 times with PBS and lysates generated using RIPA buffer. These were then

centrifuged at 15,000 *g* for 12 minutes at 4°C, and the supernatant was added to Laemmli loading buffer.

Immunoblotting was performed as previously described (23), and the blots were immunolabeled overnight with a polyclonal anti-MCM4 antibody (Abcam, targeting MCM4 exon 14, or Santa Cruz Biotechnology Inc., targeting the N terminus of MCM4, at 1:2,000 and 1:500, respectively), anti-FLAG at 1:1,000 (Sigma-Aldrich), and β-actin or GAPDH at 1:10,000 (Sigma-Aldrich) as a loading control.

Generation and validation of mouse lines
Mice used in these studies were reported previously, along with genotyping protocols (6, 7). To generate the mice analyzed here, we crossed mice of the genotypes $Mcm4^{Chaos3/Chaos3}$ and $Mcm4^{+/-}Mcm3^{+/-}$ to generate the control ($Mcm4^{Chaos3/+}Mcm3^{+/-}$) and mutant ($Mcm4^{Chaos3/-}Mcm3^{+/-}$) animals.

Mouse histology
Adult mouse adrenals were fixed in 4% paraformaldehyde (Sigma-Aldrich) and embedded in paraffin. Sections were obtained using a microtome (Leitz 1512) at 6-μm thickness, deparaffinized, and hydrated through a xylene and ethanol series. H&E staining was performed using standard procedures (25).

GATA-4 immunohistochemistry
Sections were hydrated, treated with 3% hydrogen peroxide, boiled in 10 mM sodium citrate buffer pH 6.0, blocked with 10% normal horse serum (Sigma-Aldrich), and treated with biotin blocking reagent (Vector Laboratories). They were then incubated overnight with goat anti–GATA-4 (C-20, Santa Cruz Biotechnology Inc.) diluted 1:250 in PBS Triton X-100 0.1% (T-PBS). Sections were washed in T-PBS and incubated with a biotinylated horse anti-goat secondary antibody (Vector Laboratories) diluted 1:500 in T-PBS, for 2 hours. They were washed, treated with avidin-biotin complex (ABC Elite kit, Vector Laboratories) according to the manufacturer's instructions, rinsed again, and incubated with 3-3′diaminobenzidine/nickel (Vector Laboratories). The reaction was stopped with H_2O, and slides were dehydrated and coverslipped using DPX mounting medium (Fisher). Images were acquired using a Leica DMR microscope, and digital images were captured using a Leica DC200 camera and DCViewer software (Leica).

SCC/CYP11B1 immunofluorescence
Sections were processed as above up to the blocking step, incubated with mouse anti-CYP11B1 (1:20 in T-PBS) and rabbit anti-SCC (Millipore, 1:1,000 in T-PBS). After three washes with T-PBS, slides were incubated for 2 hours with goat anti-mouse–Alexa Fluor 488 and goat anti-rabbit–Alexa Fluor 568 (Invitrogen) diluted 1:1,000 in T-PBS and, after further washes, coverslipped. Images were acquired as above.

Non-radioactive in situ hybridization
For non-radioactive in situ hybridization (NR-ISH), digoxigenin-labeled (DIG-labeled) antisense and sense Gli1 cRNA probes were synthesized by in vitro transcription in the presence of DIG-labeling mix (Roche) using approximately 1 μg of linearized template and T7 or SP6 RNA polymerase (New England BioLabs Inc.) (25). Paraffin sections were dehydrated through an ascending alcohol series and NR-ISH performed as described previously (26).

Study approval
This study was approved by the Our Lady's Children's Hospital ethics committee, and all parents (and children, when possible) gave written informed consent. All the experiments involving mice were approved by the IACUC of Cornell University.

Address correspondence to: Adrian J.L. Clark, Centre for Endocrinology, First Floor North, John Vane Science Centre, Charterhouse Square, London EC1M 6BQ, United Kingdom. Phone: 44.20.7882.6202; Fax: 44.20.7882.6197; E-mail: a.j.clark@qmul.ac.uk.

1. Shepard TH, Landing BH, Mason DG. Familial Addison's disease; case reports of two sisters with corticoid deficiency unassociated with hypoaldosteronism. *AMA J Dis Child*. 1959;97(2):154–162.
2. Clark AJ, Weber A. Adrenocorticotropin insensitivity syndromes. *Endocr Rev*. 1998;19(6):828–843.
3. O'Riordan SM, Lynch SA, Hindmarsh PC, Chan LF, Clark AJ, Costigan C. A novel variant of familial glucocorticoid deficiency prevalent among the Irish Traveler population. *J Clin Endocrinol Metab*. 2008; 93(7):2896–2899.
4. Forsburg SL. Eukaryotic MCM proteins: beyond replication initiation. *Microbiol Mol Biol Rev*. 2004; 68(1):109–131.
5. Musahl C, Schulte D, Burkhart R, Knippers R. A human homologue of the yeast replication protein Cdc21. Interactions with other Mcm proteins. *Eur J Biochem*. 1995;230(3):1096–1101.
6. Shima N, Buske TR, Schimenti JC. Genetic screen for chromosome instability in mice: Mcm4 and breast cancer. *Cell Cycle*. 2007;6(10):1135–1140.
7. Chuang CH, Wallace MD, Abratte C, Southard T, Schimenti JC. Incremental genetic perturbations to MCM2-7 expression and subcellular distribution reveal exquisite sensitivity of mice to DNA replication stress. *PLoS Genet*. 2010; 6(9):e1001110.
8. Kiiveri S, et al. Differential expression of GATA-4 and GATA-6 in fetal and adult mouse and human adrenal tissue. *Endocrinology*. 2002;143(8):3136–3143.
9. Masai H, et al. Phosphorylation of MCM4 by Cdc7 kinase facilitates its interaction with Cdc45 on the chromatin. *J Biol Chem*. 2006;281(51):39249–39261.
10. Sheu YJ, Stillman B. The Dbf4-Cdc7 kinase promotes S phase by alleviating an inhibitory activity in Mcm4. *Nature*. 2010;463(7277):113–117.
11. Shima N, et al. A viable allele of Mcm4 causes chromosome instability and mammary adenocarcinomas in mice. *Nat Genet*. 2007;39(1):93–98.
12. Li XC, Schimenti JC, Tye BK. Aneuploidy and improved growth are coincident but not causal in a yeast cancer model. *PLoS Biol*. 2009;7(7):e1000161.
13. Kim JS, Kubota H, Kiuchi Y, Doi K, Saegusa J. Subcapsular cell hyperplasia and mast cell infiltration in the adrenal cortex of mice: comparative study in 7 inbred strains. *Exp Anim*. 1997;46(4):303–306.
14. Berthon A, et al. Constitutive beta-catenin activation induces adrenal hyperplasia and promotes adrenal cancer development. *Hum Mol Genet*. 2010; 19(8):1561–1576.
15. Parviainen H, et al. GATA transcription factors in adrenal development and tumors. *Mol Cell Endocrinol*. 2007;265–266:17–22.
16. King P, Paul A, Laufer E. Shh signaling regulates adrenocortical development and identifies progenitors of steroidogenic lineages. *Proc Natl Acad Sci U S A*. 2009;106(50):21185–21190.
17. Wood MA, Hammer GD. Adrenocortical stem and progenitor cells: unifying model of two proposed origins. *Mol Cell Endocrinol*. 2010;336(1–2):206–212.
18. Pruitt SC, Bailey KJ, Freeland A. Reduced Mcm2 expression results in severe stem/progenitor cell deficiency and cancer. *Stem Cells*. 2007; 25(12):3121–3132.
19. Orange JS. Human natural killer cell deficiencies. *Curr Opin Allergy Clin Immunol*. 2006;6(6):399–409.
20. Gineau L, et al. Partial MCM4 deficiency in patients with growth retardation, adrenal insufficiency, and natural killer cell deficiency. *J Clin Invest*. doi:10.1172/JCI61014.
21. Tye BK. MCM proteins in DNA replication. *Annu Rev Biochem*. 1999;68:649–686.
22. Bicknell LS, et al. Mutations in the pre-replication complex cause Meier-Gorlin syndrome. *Nat Genet*. 2011;43(4):356–359.
23. Metherell LA, et al. Mutations in MRAP, encoding a new interacting partner of the ACTH receptor, cause familial glucocorticoid deficiency type 2. *Nat Genet*. 2005;37(2):166–170.
24. Carr IM, Sheridan E, Hayward BE, Markham AF, Bonthron DT. IBDfinder and SNPsetter: tools for pedigree-independent identification of autozygous regions in individuals with recessive inherited disease. *Hum Mutat*. 2009;30(6):960–967.
25. Guasti L, Paul A, Laufer E, King P. Localization of Sonic hedgehog secreting and receiving cells in the developing and adult rat adrenal cortex. *Mol Cell Endocrinol*. 2011;336(1–2):117–122.
26. Guasti L, et al. Expression pattern of the ether-a-go-go-related (ERG) family proteins in the adult mouse central nervous system: evidence for coassembly of different subunits. *J Comp Neurol*. 2005; 491(2):157–174.